

Steady Flow of Maxwell Fluid with Convective Boundary Conditions

Tasawar Hayat^{a,b}, Sabir Ali Shehzad^a, Muhammad Qasim^a, and Saleem Obaidat^b

^a Department of Mathematics, Quaid-i-Azam University 45320 Islamabad 44000, Pakistan

^b Department of Mathematics, College of Sciences, King Saud University P.O. Box 2455, Riyadh 11451, Saudi Arabia

Reprint requests to M. Q.; Tel.: +92 51 90642172; E-mail: mq-qau@yahoo.com

Z. Naturforsch. **66a**, 417–422 (2011); received December 6, 2010 / revised January 23, 2011

We performed a study for the flow of a Maxwell fluid induced by a stretching surface. Heat transfer is also addressed by using the convective boundary conditions. We solved the nonlinear problem by employing a homotopy analysis method (HAM). We computed the velocity, temperature, and Nusselt number. The role of embedded parameters on the velocity and temperature is particularly analyzed.

Key words: Heat Transfer; Convective Boundary Conditions; Stretching Surface.

1. Introduction

Many fluids in industry and engineering applications cannot be described by the Navier–Stokes equations. Examples of such fluids are polymer solutions, paints, certain oils, lubricants, colloidal and suspension solutions, clay coating etc. As a consequence of diverse physical structure of such fluids there is not a single model which can predict all the salient features of non-Newtonian fluids. The non-Newtonian fluids in general are classified into three categories namely the differential, rate, and integral types. There is a simplest class of rate type fluids known as Maxwell fluid. This model can easily describe the characteristics of the relaxation time. Such effects cannot be predicted in the differential type non-Newtonian fluids. The channel flow of an upper convected Maxwell (UCM) fluid induced by suction has been taken into account by Choi et al. [1]. Tan and Xu [2] investigated the flow due to a suddenly moved plate in a viscoelastic fluid with fractional Maxwell model. Fetecau et al. [3] discussed the flow of a Maxwell fluid induced by an oscillatory rigid plate. Zierep and Fetecau [4] discussed the Rayleigh–Stokes problem for a Maxwell fluid for three different types of initial and/or boundary conditions. Jamil and Fetecau [5] provided the exact solution for the helical flows of a Maxwell fluid between two infinite coaxial circular cylinders. The stability analysis of double-diffusive convection of a Maxwell fluid in a porous medium has been addressed by Wang and Tan [6]. Sadeghy et al. [7] numerically analyzed the stagnation point flow of an upper

convected Maxwell fluid. Hayat et al. [8] analyzed the magnetohydrodynamic (MHD) flow and mass transfer of a UCM fluid past a porous shrinking sheet in the presence of chemical reactive species. Qi and Xu [9] examined the unsteady flow of a fractional Maxwell fluid in a channel. Hayat and Qasim [10] carried out the analysis for the flow and mass transfer characteristics in a Maxwell fluid past a stretching sheet with thermal radiation, Ohmic dissipation, and thermophoresis.

Interest in the stretching flows subject to boundary layer approximation has now increased substantially. This is because of their extensive applications in the polymer industry and manufacturing processes including wire drawing, spinning of filaments, hot rolling, crystal growing, fiber production, paper production, and continuous casting. A closed form solution for steady flow past a stretching surface has been provided by Crane [11]. Later, the flow problems of the stretching surface have been extended in numerous ways such as to include MHD effects, heat and mass transfer, non-Newtonian fluid, suction/injection etc. Such flows are rarely discussed when the convective boundary conditions are taken into account. Aziz [12] investigated the boundary layer flow over a flat plate with convective boundary conditions. Ishak [13] generalized the flow analysis of Aziz [12] by introducing the suction and injection. Makinde and Aziz [14] investigated the MHD mixed convection flow from a vertical plate embedded in a porous medium. Very recently Yao et al. [15] discussed the stretching/shrinking wall problem in a viscous fluid.

The objective of present study is to extend the flow analysis of Yao et al. [15] from viscous to Maxwell fluid. Further our interest is to provide an analytic solution for a highly nonlinear problem. The structure of the paper is as follows. The flow problem is formulated in Section 2. Sections 3 and 4 deal with the series solutions and their convergence, respectively. Homotopy analysis method (HAM) [16–25] is used in computation of series solutions. Results and discussion are included in Section 5. Section 6 consists of conclusions.

2. Governing Problems

We consider the two-dimensional boundary layer flow of an incompressible Maxwell fluid bounded by a continuously stretching sheet with heat transfer in a stationary fluid. We adopt that the velocity of the stretching sheet is $u_w(x) = bx$, (where b is a real number). Further the constant mass transfer velocity is taken as v_w with $v_w > 0$ for injection and $v_w < 0$ for suction, respectively. The x - and y -axes in the Cartesian coordinate system are parallel and perpendicular to the sheet, respectively. The governing equations are [7, 10] and [15]

$$\frac{\partial u}{\partial x} + \frac{\partial v}{\partial y} = 0, \quad (1)$$

$$u \frac{\partial u}{\partial x} + v \frac{\partial u}{\partial y} = \nu \frac{\partial^2 u}{\partial y^2} - \lambda \left[u^2 \frac{\partial^2 u}{\partial x^2} + v^2 \frac{\partial^2 u}{\partial y^2} + 2uv \frac{\partial^2 u}{\partial x \partial y} \right], \quad (2)$$

$$u \frac{\partial T}{\partial x} + v \frac{\partial T}{\partial y} = \sigma \frac{\partial^2 T}{\partial y^2}, \quad (3)$$

in which u and v denote the velocity components in the x - and y -directions, λ the relaxation time, T the fluid temperature, σ the thermal diffusivity of the fluid, $\nu = (\mu/\rho)$ the kinematic viscosity, ρ the density of the fluid, and the viscous dissipation is not accounted.

The boundary conditions are defined as

$$u = u_w(x) = bx, \quad v = v_w, \quad (4)$$

$$-k \frac{\partial T}{\partial y} = h(T_f - T_w) \quad \text{at } y = 0,$$

$$u = 0, \quad T = T_\infty \quad \text{as } y \rightarrow \infty, \quad (5)$$

where k indicates the thermal conductivity of the fluid, h the convective heat transfer coefficient, v_w the wall heat transfer velocity, and T_f the convective fluid temperature below the moving sheet.

We introduce the similarity transformations

$$u = axf'(\eta), \quad v = -\sqrt{av}f(\eta), \quad (6)$$

$$\theta(\eta) = \frac{T - T_\infty}{T_f - T_\infty}, \quad \eta = y\sqrt{\frac{a}{\nu}}.$$

Here a is a constant and prime denotes the differentiation with respect to η .

Equations (2)–(5) yield

$$f''' + ff'' - f'^2 + \beta(2ff'f'' - f^2f''') = 0, \quad (7)$$

$$\theta'' + \text{Pr}f\theta' = 0, \quad (8)$$

$$f = S, \quad f' = b/a = \alpha, \quad (9)$$

$$\theta' = -\gamma(1 - \theta(0)) \quad \text{at } \eta = 0, \quad (10)$$

$$f' = 0, \quad \theta = 0 \quad \text{as } \eta = \infty,$$

where (1) is satisfied automatically; $\beta = \lambda a$ is the Deborah number, $S = -\frac{v_w}{\sqrt{av}}$ is the suction parameter, $\alpha = \frac{b}{a}$ is a parameter, $\text{Pr} = \frac{\nu}{\sigma}$ is the Prandtl number, $\gamma = \frac{h}{k}\sqrt{\frac{\nu}{a}}$ is the Biot number, a is a constant, and prime shows differentiation with respect to η .

The expression of the local Nusselt number Nu_x is

$$\text{Nu}_x = \frac{xq_w}{k(T_w - T_\infty)}, \quad (11)$$

where the heat transfer q_w is defined as

$$q_w = -k \left(\frac{\partial T}{\partial y} \right)_{y=0}. \quad (12)$$

In dimensionless scale, (11) becomes

$$\text{Nu}/\text{Re}_x^{1/2} = -\theta'(0).$$

3. Homotopy Analysis Solutions

We express f and θ by a set of base functions

$$\{\eta^k \exp(-n\eta), \quad k \geq 0, n \geq 0\} \quad (13)$$

as follows:

$$f(\eta) = \sum_{n=0}^{\infty} \sum_{k=0}^{\infty} a_{m,n}^k \eta^k \exp(-n\eta), \quad (14)$$

$$\theta(\eta) = \sum_{n=0}^{\infty} \sum_{k=0}^{\infty} b_{m,n}^k \eta^k \exp(-n\eta), \quad (15)$$

in which $a_{m,n}^k$ and $b_{m,n}^k$ are the coefficients. We further select the following initial approximations and auxiliary linear operators:

$$f_0(\eta) = S + \alpha(1 - e^{-\eta}), \quad \theta_0(\eta) = \frac{\gamma \exp(-\eta)}{1 + \gamma}, \quad (16)$$

$$\mathcal{L}_f = f''' - f', \quad \mathcal{L}_\theta = \theta'' - \theta, \quad (17)$$

with

$$\begin{aligned} \mathcal{L}_f(C_1 + C_2 e^\eta + C_3 e^{-\eta}) &= 0, \\ \mathcal{L}_\theta(C_4 e^\eta + C_5 e^{-\eta}) &= 0, \end{aligned} \quad (18)$$

where C_i ($i = 1-5$) denote the arbitrary constants.

The associated zeroth-order deformation problems are

$$(1-p)\mathcal{L}_f[\hat{f}(\eta; p) - f_0(\eta)] = p h_f \mathcal{N}_f[\hat{f}(\eta; p)], \quad (19)$$

$$(1-p)\mathcal{L}_\theta[\hat{\theta}(\eta; p) - \theta_0(\eta)] = p h_\theta \mathcal{N}_\theta[\hat{f}(\eta; p), \hat{\theta}(\eta; p)], \quad (20)$$

$$\begin{aligned} \hat{f}(0; p) &= S, \quad \hat{f}'(0; p) = b/a = \alpha, \quad \hat{f}'(\infty; p) = 0, \\ \hat{\theta}(0, p) &= -\gamma[1 - \theta(0, p)], \quad \hat{\theta}(\infty, p) = 0, \end{aligned} \quad (21)$$

$$\begin{aligned} \mathcal{N}_f[\hat{f}(\eta, p)] &= \frac{\partial^3 \hat{f}(\eta, p)}{\partial \eta^3} - \hat{f}(\eta, p) \frac{\partial^2 \hat{f}(\eta, p)}{\partial \eta^2} \\ &\quad - \left(\frac{\partial \hat{f}(\eta, p)}{\partial \eta} \right)^2 + \beta \left[2\hat{f}(\eta, p) \frac{\partial \hat{f}(\eta, p)}{\partial \eta} \right. \\ &\quad \left. \cdot \frac{\partial^2 \hat{f}(\eta, p)}{\partial \eta^2} - (\hat{f}(\eta, p))^2 \frac{\partial^3 \hat{f}(\eta, p)}{\partial \eta^3} \right], \end{aligned} \quad (22)$$

$$\begin{aligned} \mathcal{N}_\theta[\hat{\theta}(\eta, p), \hat{f}(\eta, p)] &= \\ \frac{\partial^2 \hat{\theta}(\eta, p)}{\partial \eta^2} &+ \text{Pr} \hat{f}(\eta, p) \frac{\partial \hat{\theta}(\eta, p)}{\partial \eta}. \end{aligned} \quad (23)$$

Here p is an embedding parameter, h_f and h_θ are the non-zero auxiliary parameters and \mathcal{N}_f and \mathcal{N}_θ the non-linear operators.

Note that for $p = 0$ and $p = 1$ we have

$$\begin{aligned} \hat{f}(\eta; 0) &= f_0(\eta), \quad \hat{\theta}(\eta, 0) = \theta_0(\eta) \text{ and} \\ \hat{f}(\eta; 1) &= f(\eta), \quad \hat{\theta}(\eta, 1) = \theta(\eta), \end{aligned} \quad (24)$$

and when p increases from 0 to 1 then $f(\eta, p)$ and $\theta(\eta, p)$ varies from $f_0(\eta), \theta_0(\eta)$ to $f(\eta)$ and $\theta(\eta)$.

In view of Taylor's series one can expand

$$f(\eta, p) = f_0(\eta) + \sum_{m=1}^{\infty} f_m(\eta) p^m, \quad (25)$$

$$\theta(\eta, p) = \theta_0(\eta) + \sum_{m=1}^{\infty} \theta_m(\eta) p^m, \quad (26)$$

$$f_m(\eta) = \frac{1}{m!} \left. \frac{\partial^m f(\eta; p)}{\partial p^m} \right|_{p=0}, \quad (27)$$

$$\theta_m(\eta) = \frac{1}{m!} \left. \frac{\partial^m \theta(\eta; p)}{\partial p^m} \right|_{p=0},$$

where the convergence of above series strongly depends upon h_f and h_θ . Considering that h_f and h_θ are selected properly so that (25) and (26) converge at $p = 1$ and thus one has

$$f(\eta) = f_0(\eta) + \sum_{m=1}^{\infty} f_m(\eta), \quad (28)$$

$$\theta(\eta) = \theta_0(\eta) + \sum_{m=1}^{\infty} \theta_m(\eta). \quad (29)$$

The problems at m th-order are

$$\mathcal{L}_f[f_m(\eta) - \chi_m f_{m-1}(\eta)] = h_f \mathcal{R}_f^m(\eta), \quad (30)$$

$$\mathcal{L}_\theta[\theta_m(\eta) - \chi_m \theta_{m-1}(\eta)] = h_\theta \mathcal{R}_\theta^m(\eta), \quad (31)$$

$$\begin{aligned} f_m(0) &= f'_m(0) = f'_m(\infty) = 0, \\ \theta'_m(0) - \gamma \theta_m(0) &= \theta_m(\infty) = 0, \end{aligned} \quad (32)$$

$$\begin{aligned} \mathcal{R}_f^m(\eta) &= f_{m-1}'''(\eta) + \sum_{k=0}^{m-1} [f_{m-1-k} f_k'' - f_{m-1-k}' f_k'''] \\ &\quad + \beta \sum_{k=0}^{m-1} f_{m-1-k} \sum_{l=0}^k [2f_{k-l}' f_l'' - f_{k-l} f_l'''], \end{aligned} \quad (33)$$

$$\mathcal{R}_\theta^m(\eta) = \theta_{m-1}''(\eta) + \text{Pr} \sum_{k=0}^{m-1} \theta_{m-1-k}' f_k, \quad (34)$$

$$\chi_m = \begin{cases} 0, & m \leq 1, \\ 1, & m > 1. \end{cases} \quad (35)$$

The general solutions can be expressed in the forms

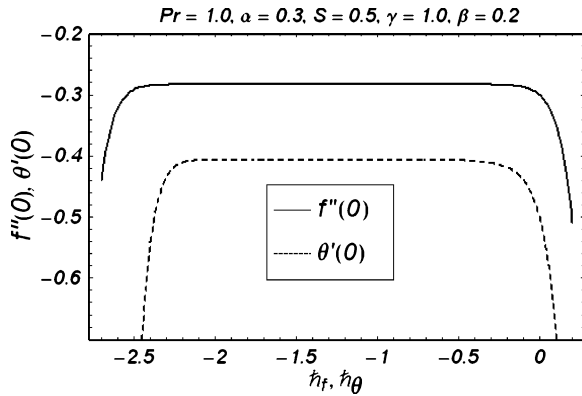
$$f_m(\eta) = f_m^*(\eta) + C_1 + C_2 e^\eta + C_3 e^{-\eta}, \quad (36)$$

$$\theta_m(\eta) = \theta_m^*(\eta) + C_4 e^\eta + C_5 e^{-\eta} \quad (37)$$

in which f_m^* and θ_m^* indicate the special solutions.

4. Convergence of the Homotopy Solutions

Clearly, the expressions (28) and (29) contain the non-zero auxiliary parameters h_f and h_θ which can ad-

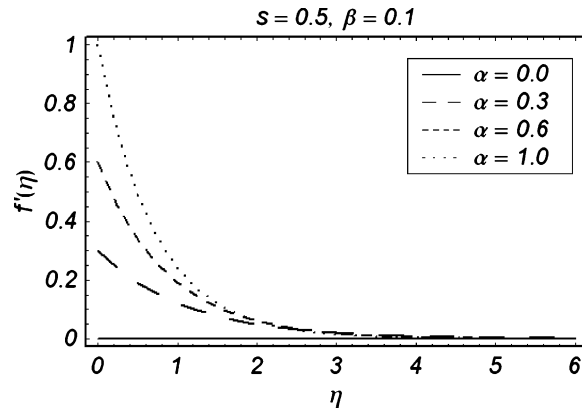
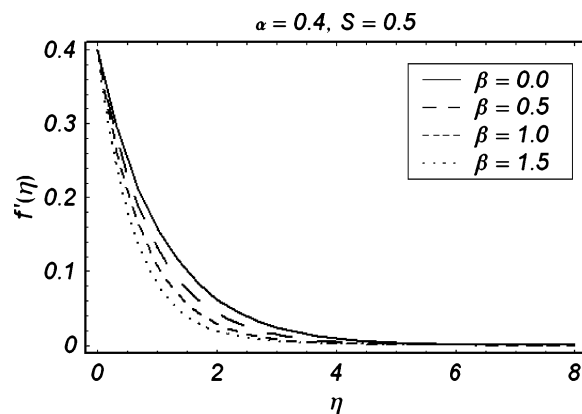
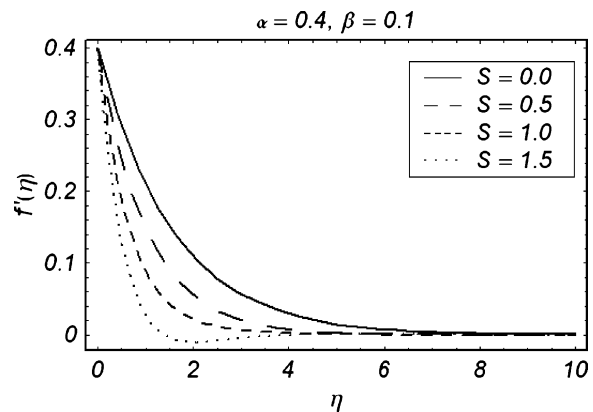
Fig. 1. h -curves for f and θ .Table 1. Convergence of the homotopy solution for different order of approximations when $\beta = 0.2$, $\alpha = 0.3$, $Pr = 1.0$, $S = 0.5$, $\gamma = 1.0$, and $h_f = h_\theta = -1.4$.

Order of approximation	$-f''(0)$	$-\theta'(0)$
1	0.2829900	0.4300000
5	0.2814982	0.4064811
10	0.2814950	0.4047923
20	0.2814950	0.4046587
30	0.2814950	0.4046572
35	0.2814950	0.4046572
40	0.2814950	0.4046572

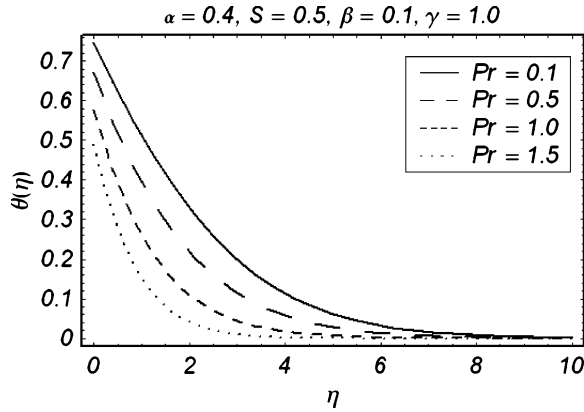
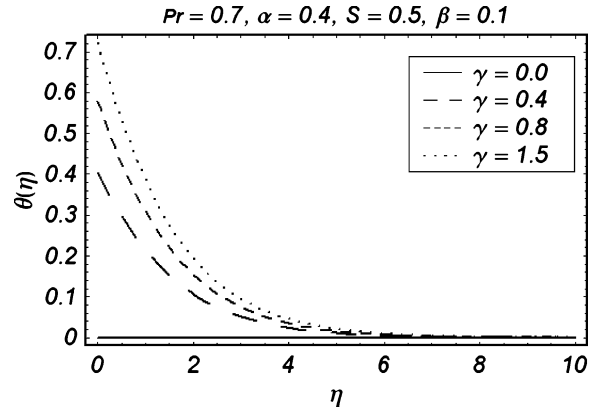
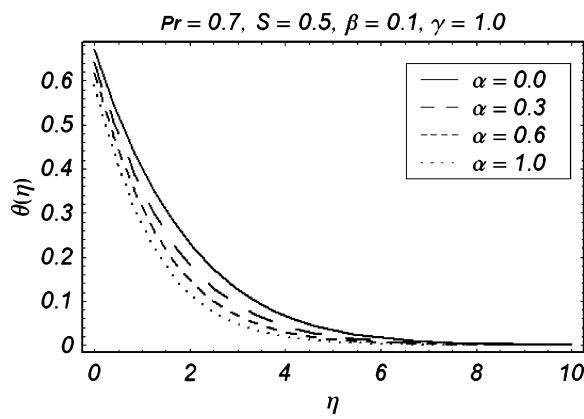
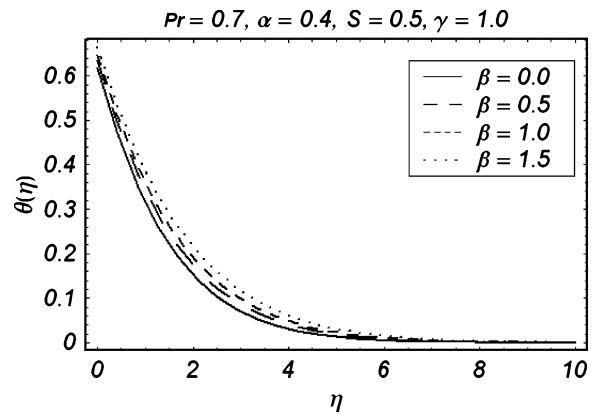
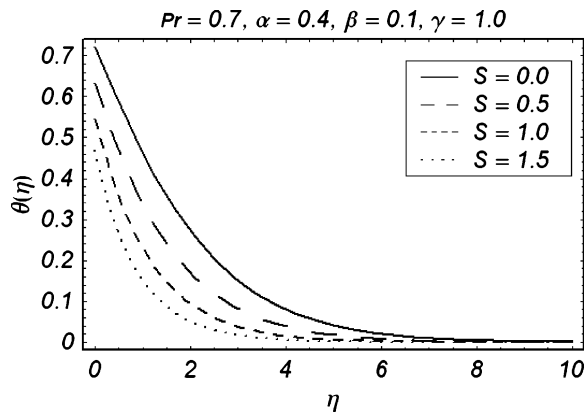
just and control the convergence of the homotopy solutions. For the range of admissible values of h_f and h_θ , the h -curves have been portrayed for 20th-order of approximations. Figure 1 shows that the range of admissible values of h_f and h_θ are $-2.4 \leq h_f \leq -0.2$ and $-2.1 \leq h_\theta \leq -0.4$. The series converges in the whole region of η when $h_f = h_\theta = -1.4$.

5. Graphical Results and Discussion

In this section our main interest is to discuss the influence of emerging parameters such as stretching parameter α , Deborah number β , suction parameter S , Prandtl number Pr , and Biot number γ on the velocity and temperature fields. The analysis of such variations is made through Figures 2–9. Figures 2–4 are displayed to see the effects of α , β , and S on the velocity field f' . As α increases in Figure 2, the flow velocity increases. Figure 3 shows the effects of β on f' . It is obvious from this figure that f' is a decreasing function of β . The same behaviour is observed as the suction parameter S increases in Figure 4. It is seen that the boundary layer thickness decreases with increasing values of $S > 0$. Figures 5–9 depict the influences of

Fig. 2. Influence of α on f' .Fig. 3. Influence of β on f' .Fig. 4. Influence of S on f' .

Pr , α , S , γ , and β on the temperature profile θ . Figure 5 describes the effects of Pr on θ . Here θ decreases when Pr increases. Figure 6 indicates that θ is a decreasing

Fig. 5. Influence of Pr on θ .Fig. 8. Influence of γ on θ .Fig. 6. Influence of α on θ .Fig. 9. Influence of β on θ .Fig. 7. Influence of S on θ .

function of α . In Figure 7 the variation of temperature θ is plotted for the different values of S . The temperature profile decreases by increasing S . Figure 8 shows

Table 2. Values of the local Nusselt number $Nu/Re_x^{1/2}$ for the parameters Pr , γ , and α when $S = 0.5$ and $\beta = 0.2$.

Pr	γ	α	$Nu/Re_x^{1/2}$
0.5	1.0	0.1	0.23336
1.0			0.36588
1.5			0.45796
2.0			0.52558
1.0	0.0		0.3189
	0.5		0.26799
	1.0		0.36591
	2.0		0.2039
		0.1	0.36588
		0.3	0.40466
		0.8	0.45825
		1.0	0.47254

the influence of the Biot number γ on θ . Temperature field increases by increasing γ . Figure 9 is plotted to see the effects of β on temperature profile θ . It can

been seen from this figure that the temperature is an increasing function of β .

6. Concluding Remarks

In this work, we consider the effects of heat transfer on the flow of a Maxwell fluid over a stretching wall with prescribed boundary conditions. The homotopy analysis method has been applied to find the series solutions. The graphical results are discussed to see the effects of interesting parameters. The main results are as follows:

- By increasing α , the velocity field f' increases.
- The velocity profile f' decreases by increasing Deborah number β and suction parameter S .
- Increase in Prandtl number decrease the temperature profile θ .
- The effects of Biot number γ and Deborah number β on θ are similar in a qualitative sense.

Acknowledgements

The first author (as a visiting Professor) thanks the King Saud university of Saudi Arabia for the support via KSU-VPP-117.

- [1] J. J. Choi, Z. Rusak, and J. A. Tichy, *J. Non-Newtonian Fluid Mech.* **85**, 165 (1999).
- [2] W. C. Tan and M. Y. Xu, *Acta Mech. Sin.* **18**, 342 (2002).
- [3] C. Fetecau, M. Jamil, C. Fetecau, and I. Siddique, *Int. J. Nonlin. Mech.* **44**, 1085 (2009).
- [4] J. Zierep and C. Fetecau, *Int. J. Eng. Sci.* **45**, 617 (2007).
- [5] M. Jamil and C. Fetecau, *Nonlin. Anal.: Real World Appl.* **11**, 4302 (2010).
- [6] S. Wang and W. C. Tan, *Phys. Lett. A* **372**, 3046 (2008).
- [7] K. Sadeghy, A. H. Najafi, and M. Saffaripour, *Int. J. Nonlin. Mech.* **40**, 1220 (2005).
- [8] T. Hayat, Z. Abbas, and N. Ali, *Phys. Lett. A* **372**, 4698 (2008).
- [9] H. Qi and M. Xu, *Mech. Res. Commun.* **34**, 210 (2007).
- [10] T. Hayat and M. Qasim, *Int. J. Heat Mass Transf.* **53**, 4780 (2010).
- [11] L. J. Crane, *Z. Angew. Math. Phys.* **21**, 645 (1970).
- [12] A. Aziz, *Commun. Nonlin. Sci. Numer. Simul.* **14**, 1064 (2009).
- [13] A. Ishak, *Appl. Math. Comput.* **217**, 837 (2010).
- [14] O. D. Makinde and A. Aziz, *Int. J. Therm. Sci.* **49**, 1813 (2010).
- [15] S. Yao, T. Fang, and Y. Zhong, *Commun. Nonlin. Sci. Numer. Simul.* **16**, 752 (2011).
- [16] S. J. Liao, *Beyond Perturbation: Introduction to Homotopy Analysis Method*, Chapman and Hall, CRC Press, Boca Raton 2003.
- [17] S. J. Liao, *Stud. Appl. Math.* **117**, 2529 (2006).
- [18] T. Hayat, M. Qasim, and Z. Abbas, *Commun. Nonlin. Sci. Numer. Simul.* **15**, 2375 (2010).
- [19] N. F. M. Noor and I. Hashim, *Int. J. Heat Mass Transf.* **53**, 2044 (2010).
- [20] T. Hayat, M. Qasim, and Z. Abbas, *Z. Naturforsch.* **64a**, 231 (2010).
- [21] N. Kousar and S. J. Liao, *Transp. Porous Media* **83**, 397 (2010).
- [22] T. Hayat, K. Maqbool, and S. Asghar, *Z. Naturforsch.* **64a**, 769 (2009).
- [23] S. J. Liao, *Commun. Nonlin. Sci. Numer. Simul.* **14**, 2144 (2009).
- [24] T. Hayat and M. Qasim, *Z. Naturforsch.* **64a**, 950 (2010).
- [25] T. Hayat, M. Qasim, Z. Abbas, and A. A. Hendi, *Z. Naturforsch.* **64a**, 1111 (2010).